



# **Lateral Semicircular Canal Asymmetry in Idiopathic Scoliosis: An Early Link between Biomechanical, Hormonal and Neurosensory Theories?**

Martin Hitier, Michèle Hamon, Pierre Denise, Julien Lacoudre, Marie-Aude Thenint, Jean-François Mallet, Sylvain Moreau, Gaëlle Quarck

## **► To cite this version:**

Martin Hitier, Michèle Hamon, Pierre Denise, Julien Lacoudre, Marie-Aude Thenint, et al.. Lateral Semicircular Canal Asymmetry in Idiopathic Scoliosis: An Early Link between Biomechanical, Hormonal and Neurosensory Theories?. PLoS ONE, 2015, 10 (7), pp.e0131120. 10.1371/journal.pone.0131120 . hal-02190877

**HAL Id: hal-02190877**

**<https://normandie-univ.hal.science/hal-02190877>**

Submitted on 18 Sep 2019

**HAL** is a multi-disciplinary open access archive for the deposit and dissemination of scientific research documents, whether they are published or not. The documents may come from teaching and research institutions in France or abroad, or from public or private research centers.

L'archive ouverte pluridisciplinaire **HAL**, est destinée au dépôt et à la diffusion de documents scientifiques de niveau recherche, publiés ou non, émanant des établissements d'enseignement et de recherche français ou étrangers, des laboratoires publics ou privés.



Distributed under a Creative Commons Attribution 4.0 International License

RESEARCH ARTICLE

# Lateral Semicircular Canal Asymmetry in Idiopathic Scoliosis: An Early Link between Biomechanical, Hormonal and Neurosensory Theories?

Martin Hitier<sup>1,2,3,4\*</sup>, Michèle Hamon<sup>5</sup>, Pierre Denise<sup>4</sup>, Julien Lacoudre<sup>1</sup>, Marie-Aude Thenint<sup>5</sup>, Jean-François Mallet<sup>6</sup>, Sylvain Moreau<sup>1,2</sup>, Gaëlle Quarck<sup>4</sup>

**1** Department of Otolaryngology—Head and Neck Surgery, CHU de Caen, Caen, F-14000, France, **2** Department of Anatomy, UNICAEN, Caen, 14032, France, **3** Department of Pharmacology and Toxicology; School of Medical Sciences and Brain Health Research Center, University of Otago, Dunedin, New Zealand, **4** U 1075 COMETE, INSERM, Caen, 14032, France, **5** Department of Neuroradiology, CHU de Caen, Caen, 14000, France, **6** Department of Paediatric surgery, CHU de Caen, Caen, 14000, France

\* [mart1\\_hit@yahoo.fr](mailto:mart1_hit@yahoo.fr)



## OPEN ACCESS

**Citation:** Hitier M, Hamon M, Denise P, Lacoudre J, Thenint M-A, Mallet J-F, et al. (2015) Lateral Semicircular Canal Asymmetry in Idiopathic Scoliosis: An Early Link between Biomechanical, Hormonal and Neurosensory Theories? PLoS ONE 10(7): e0131120. doi:10.1371/journal.pone.0131120

**Editor:** Manabu Sakakibara, Tokai University, JAPAN

**Received:** January 4, 2015

**Accepted:** May 28, 2015

**Published:** July 17, 2015

**Copyright:** © 2015 Hitier et al. This is an open access article distributed under the terms of the [Creative Commons Attribution License](https://creativecommons.org/licenses/by/4.0/), which permits unrestricted use, distribution, and reproduction in any medium, provided the original author and source are credited.

**Data Availability Statement:** All relevant data are within the paper and its Supporting Information file.

**Funding:** This research was supported by a Marie Curie International Research Staff Exchange Scheme Fellowship within the 7th European Community Framework Program #918980, and Emergence Program (N° 11P03919 /11P03921) Basse-Normandie Région. The funders had no role in study design, data collection and analysis, decision to publish, or preparation of the manuscript.

**Competing Interests:** The authors have declared that no competing interests exist.

## Abstract

### Introduction

Despite its high incidence and severe morbidity, the physiopathogenesis of adolescent idiopathic scoliosis (AIS) is still unknown. Here, we looked for early anomalies in AIS which are likely to be the cause of spinal deformity and could also be targeted by early treatments. We focused on the vestibular system, which is suspected of acting in AIS pathogenesis and which exhibits an end organ with size and shape fixed before birth. We hypothesize that, in adolescents with idiopathic scoliosis, vestibular morphological anomalies were already present at birth and could possibly have caused other abnormalities.

### Materials and Methods

The vestibular organ of 18 adolescents with AIS and 9 controls were evaluated with MRI in a prospective case controlled study. We studied lateral semicircular canal orientation and the three semicircular canal positions relative to the midline. Lateral semicircular canal function was also evaluated by vestibulonystagmography after bithermal caloric stimulation.

### Results

The left lateral semicircular canal was more vertical and further from the midline in AIS ( $p = 0.01$ ) and these two parameters were highly correlated ( $r = -0.6$ ;  $p = 0.02$ ). These morphological anomalies were associated with functional anomalies in AIS (lower excitability, higher canal paresis), but were not significantly different from controls ( $p > 0.05$ ).

## Conclusion

Adolescents with idiopathic scoliosis exhibit morphological vestibular asymmetry, probably determined well before birth. Since the vestibular system influences the vestibulospinal pathway, the hypothalamus, and the cerebellum, this indicates that the vestibular system is a possible cause of later morphological, hormonal and neurosensory anomalies observed in AIS. Moreover, the simple lateral SCC MRI measurement demonstrated here could be used for early detection of AIS, selection of children for close follow-up, and initiation of preventive treatment before spinal deformity occurs.

## Introduction

Adolescent idiopathic scoliosis (AIS) is characterized by a spinal deformity of unknown origin and affects 3% of children between the ages of 10 and 16 worldwide [1–4] [1,2], resulting in pain, poor self image with social consequences, and the possible burden of heavy treatment with a brace or spine surgery [3,5]. Even if the level of proof is currently weak [6], the spinal deformity is often associated with other morphological (e.g. ribs, pelvis, arms, skull) [7–10], hormonal (e.g. leptin, melatonin signaling) [11–13], and neurosensory anomalies (e.g. vestibular, neurosensory integration) [14–17]. Authors have identified genes [18–23] and suspected environmental factors [24,25], and have elaborated theories to link these factors to the anomalies (for review see [26–28]). However, the pathogenesis of AIS remains unknown and is probably multifactorial [29].

One main difficulty is that some anomalies could be either the cause or the consequence of others. For example, the spinal deformity could be the cause or the consequence of limb asymmetry, or both could be the result of a common cause [27]. Spine deformity could also be the consequence of brain anomalies [30,31] or its causes, with the brain trying to compensate for the postural instability [32].

One strategy to be used to clarify the pathogenesis would be to establish the chronology of AIS anomalies. This could help to identify causes of AIS, which should be those that appear earliest. Ultimately, this chronology may help to design new treatments early enough to stop the disease at the earliest stage.

Here, we propose establishing a chronologic landmark in the vestibular system. Several studies argue for a vestibular impairment in AIS [14,15,33]. Additionally, vestibular lesion in guinea pigs or *Xenopus* have reproduced scoliosis, which indicates that the vestibule is a possible cause of AIS [34,35]. The mechanism of vestibular induced scoliosis is more likely an asymmetry of the vestibulospinal pathway leading to an imbalance in paraspinal muscles. Most notably, the size and shape of the vestibular organ are fixed by the ossification of the otic capsule before birth, much as a fossil in rock [36–43]. Therefore, the shape of the adolescent vestibule (i.e. bony labyrinth) is thought to be similar to the shape exhibited at birth. We thus propose studying the AIS labyrinth to determine early malformation. More precisely, we focused on the lateral semicircular canal (SCC) which can be both visualized by MRI and examined by a caloric test, allowing the evaluation of the right and left sides independently [44]. The lateral SCC is most frequently affected by malformation in the general population, probably because it is the last to be formed and ossified [45]. We hypothesized that in AIS, the lateral SCC could present early orientation troubles associated with functional impairment.

## Patients and Method

We conducted a prospective case-control study including 18 cases of idiopathic scoliosis and 9 controls approved by the Nord Ouest III Ethics Committee (approval no. 2008 A00598-47). Because all cases and controls were minor, informed written consents were obtained from their parents, caretakers or guardians. One individual gave written informed consent (as outlined in PLoS consent form) to publish the image in [Fig 1](#), [Fig 2](#) and [Fig 3](#) of this manuscript.

## Participants

Inclusion criteria for the scoliosis group included females and males 10–18 years of age presenting untreated idiopathic scoliosis with a Cobb angle between 10 and 50°. The types of scoliosis were determined according to the definition of the Scoliosis Research Society: the maximum convexity (i.e. apex) gives the side (right or left) and the location of the scoliosis. An

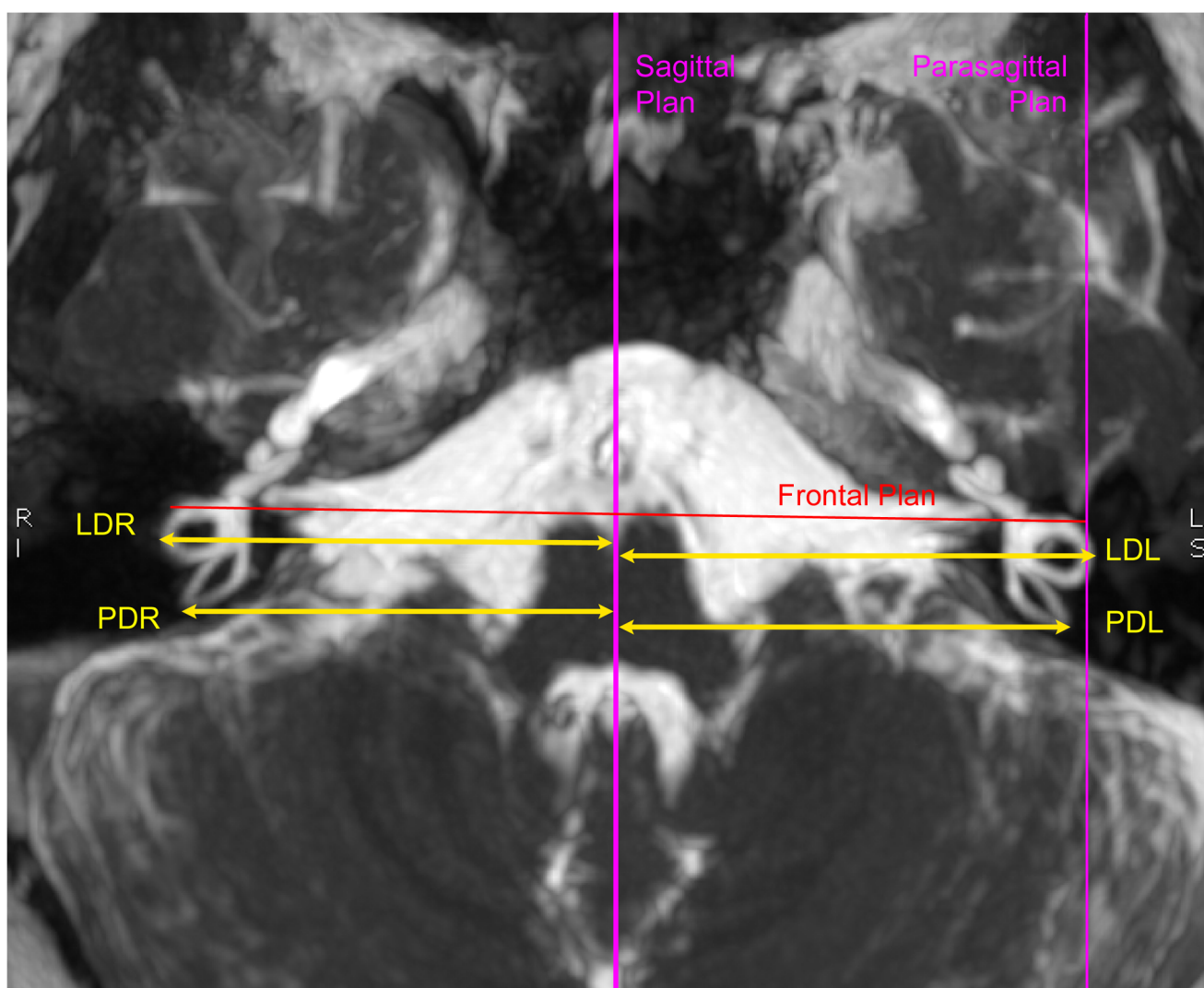


**Fig 1. Definition of planes and semicircular canal position measurements.** T2 3D MRI showing sagittal, parasagittal, and frontal planes. Distances of the semicircular canal are defined as: “lateral distance right” (LDR) for the right lateral canal, “lateral distance left” (LDL) for the left lateral canal, “posterior distance right” for the right posterior canal (PDR), and “posterior distance left” (PDL) for the left posterior canal.

doi:10.1371/journal.pone.0131120.g001

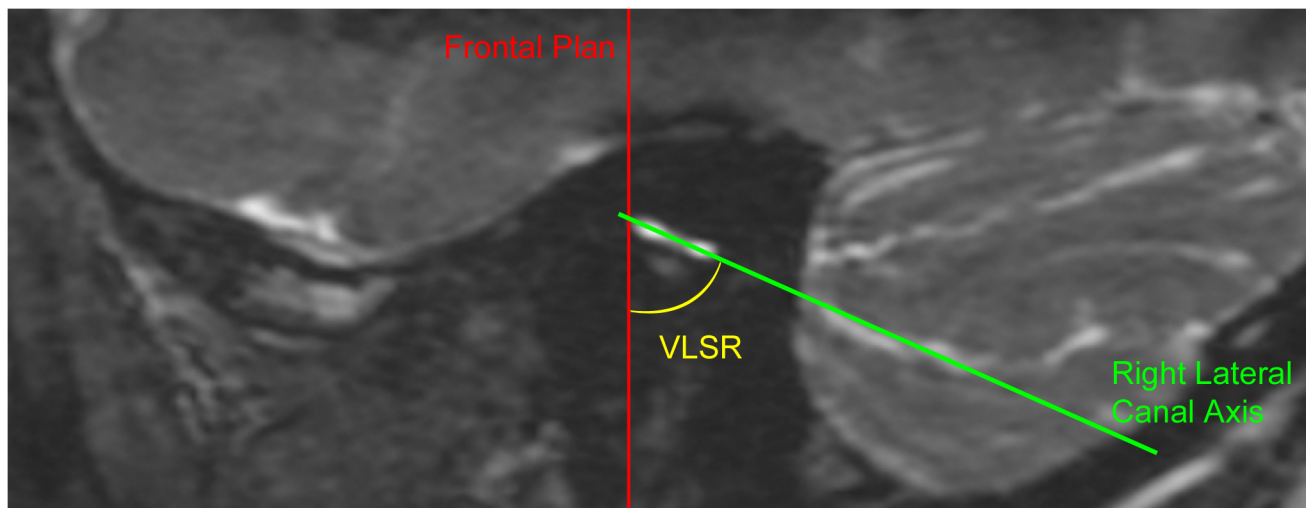


**Fig 2. Measurement of lateral semicircular canal orientation in the parasagittal plane.** T2 MRI image in the parasagittal plane showing the “Vertical Lateral canal Sagittal angle Right” (VLSR) formed between the right lateral semicircular canal and the vertical (represented by the frontal plane).

doi:10.1371/journal.pone.0131120.g002

apex located between T2 vertebra and T11-T12 disc defined thoracic scoliosis, between T12 and L1 thoracolumbar scoliosis and between L1-L2 discs and L4 lumbar scoliosis[46]. Controls consisted of adolescents recruited in the same school environment as scoliosis participants, but with no particular medical history. Exclusion criteria for both groups were: non-idiopathic scoliosis, medical history of orthopedic, endocrine, neurologic, or ear disease. Each participant (scoliosis or control) was assessed by an orthopedic surgeon (JFM), with evaluation of the scoliosis location, orientation, and severity (i.e. Cobb angle on X-ray). An ENT specialist (JL) also performed an otoscopy, a tympanometry, and tonal audiometry exams.

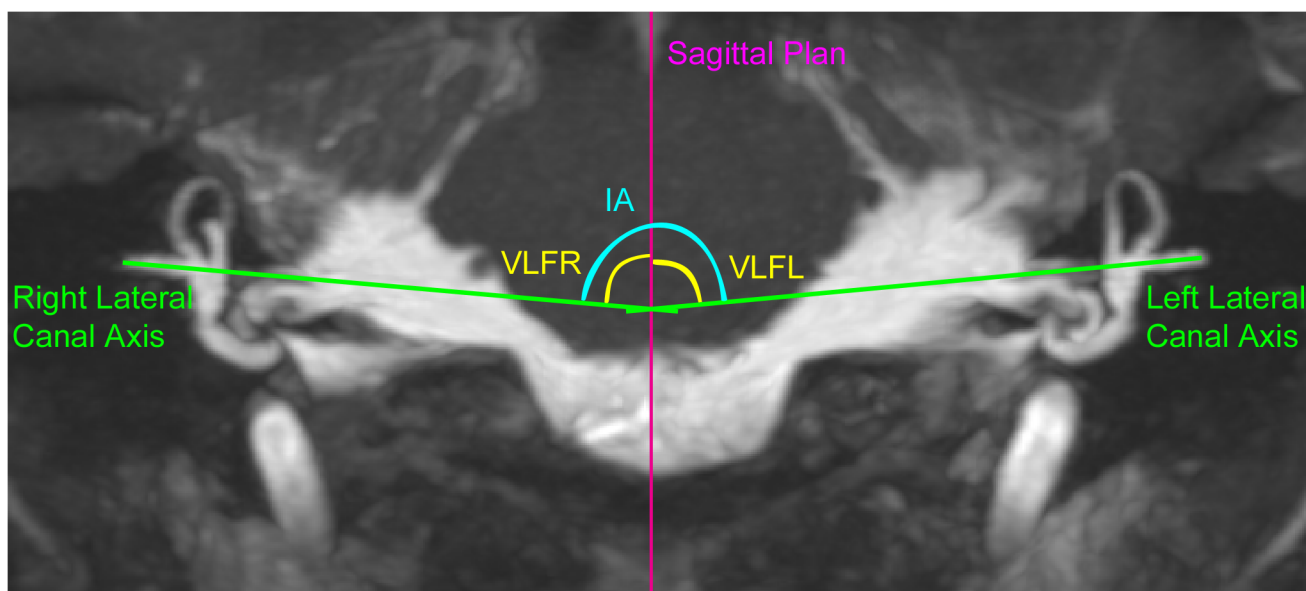


**Fig 3. Measurement of the lateral semicircular canal in the frontal plane.** MRI image in the frontal plane showing the “Intercanal Angle”(IA) formed by the axis of the right and left lateral canals; the “Vertical Lateral canal Frontal angle Right”(VLFR) formed between the right lateral SCC and the vertical axis (defined by the sagittal plane); and the “Vertical Lateral canal Frontal angle Left”(VLFL) formed between the left lateral SCC and the vertical axis.

doi:10.1371/journal.pone.0131120.g003

## Radioanatomic measurements

We used 1.5T MRI (General Electric) as a non irradiating imaging technique, with a T2 3D FastSpin Echo acquisition (scan time = 3 500 ms; echo time = 110 ms; and slice thickness = 0.5 mm). We have used a field of view (i.e. FOV) measuring 180 mm X 180 mm with a slice thickness of 0.6 mm and a matrix of 288 X 288. The resulting voxel sized 0.6 X 0.6 x 0.6 mm<sup>3</sup>. Further interpolation allows one to reduce the voxel to 0.3 X 0.3 X 0.6 mm<sup>3</sup>.

Orientation of the lateral SCC in the parasagittal and the frontal plane was analyzed by two different neuroradiologists blinded to one another and to the study group.

## Plane definition

The sagittal plane was defined according to fixed neuroanatomic median landmarks (e.g. the mesencephalic aqueduct, the 4<sup>th</sup> ventricle, the anterior median fissure). The right and left parasagittal planes are the 2 planes parallel to the sagittal plane running through the right and left lateral SCC, respectively. The frontal plane is defined as perpendicular to the sagittal and parasagittal planes ([Fig 1](#)).

## Analysis in the parasagittal plane

We evaluated the orientation of the lateral SCC in the parasagittal plane compared to the vertical axis. The vertical axis was defined as the frontal plane running through the most anterior part of the lateral SCC. We called the angle formed between the vertical and the lateral SCC the Vertical Lateral canal Sagittal angle: VLSR for the right canal and VLSL for the left ([Fig 2](#)).

## Analysis in the frontal plane

We evaluated the orientation of the lateral SCC in the frontal plane by means of both its angle with the vertical axis and the angle between the 2 lateral SCC: the angle between the lateral SCC and the vertical axis (defined by the sagittal plane) was called the Vertical Lateral canal Frontal angle: VLFR for the right SCC, and VLFL for the left. The angle between the right lateral SCC and the left lateral SCC was called the Intercanal Angle (IA) ([Fig 3](#)).

## Position of the three semi circular canals

We assessed the position of the most lateral point of the lateral SCC (i.e. LCSl defined by [\[42\]](#)) from the sagittal plane. We called this measure the Lateral Distance: LDR for the right lateral SCC, and LDL for the left SCC.

Similarly, the distance of the most posterior part of the posterior SCC from the sagittal plane was called the Posterior Distance: PDR for the right posterior SCC and PDL for the left. The the distance of the most superior part of the anterior SCC was called the *Anterior Distance*: ADR for the right anterior SCC, and ADL for the left. ([Fig 1](#)).

## Morphologic asymmetry

We evaluated the asymmetry between the right and left vestibule by comparing the difference between measures from the right side and measures from the left side (e.g. VLFR-VLFL). This analysis takes into account the side of the asymmetry. Right asymmetry will result in a positive value and left asymmetry results in negative values. Additionally, we evaluated the absolute asymmetry, which is the asymmetry regardless of the side. The absolute asymmetry of a morphologic parameter is calculated by the absolute difference between the right and the left parameters (e.g. [VLFR-VLFL]).



## Caloric test

The function of the lateral SCC was evaluated by vestibulonystagmography after alternate bin-aural bithermal caloric stimulation (250 mL warm water at 44°C for 30 s followed by 250 mL cold water at 30°C for 30 s) [47]. We used a VNG Ulmer-Synopsis device to evaluate the vestibular excitability, the directional preponderance, and the canal paresis index.

Among these three parameters, the canal paresis index is the only one which compares the function of the right and left lateral SCC (normal <15%) [48–50]. Additionally, the directional preponderance indicates stronger nystagmus beats in one side, independently of which lateral SCC is stimulated (normal <2°/s) [48–50].

## Types of comparison

We compared the morphologic parameters (angles or distances) and the functional parameters between scoliosis and control groups.

We also observed the scoliosis group for associations between the side of the scoliosis and asymmetry of morphologic or functional vestibular parameters. We then searched for correlations between the degree of scoliosis (i.e. Cobb angle) and morphologic (i.e. orientation and position) or functional (i.e. caloric test) vestibular parameters.

Finally, we studied relations between morphologic and functional vestibular parameters.

## Statistical analysis

Comparison between sex ratio and age in scoliosis and control groups were tested by Pearson's chi-square test and a *t*-test, respectively. Both radiologists' measurements were compared using a *t*-test to check for non significant differences. Then, analysis was done using the means of the two radiologists' measurements. Outliers were identified using the Hoaglin method [51]. We compared scoliosis and control groups for morphologic and functional vestibular parameters with a *t*-test or a Mann-Whitney U test depending on the distribution of each parameter. Effect size was calculated with the Pearson product-moment correlation coefficient (*r*) after the *t*-test, or as:  $r = Z / \sqrt{N}$ , after the Mann-Whitney U test. We used Fisher's exact test to compare the normality of vestibular function because there was only 1 case (i.e. fewer than 5 cases) of abnormal vestibular function in the control group. We used one-way ANOVA to compare the 3 types of scoliosis location for morphologic and functional vestibular parameters. The same method was used for the 3 types of scoliosis lateralization (right scoliosis, left scoliosis, double side scoliosis). Comparison combining both scoliosis location and side was done by two-ways ANOVA. Comparison between side of scoliosis and side of morphologic or functional asymmetry was assessed with Pearson's chi-square test. We analyzed correlations between vestibular morphologic parameters and Cobb angle, or functional vestibular parameters using Pearson correlation method or Spearman Rank correlation depending of the parameter distribution. We used two-way ANOVA to compare morphologic and functional vestibular associations between scoliosis and control groups.

All analyses were carried out with SPSS software (IBM SPSS statistic 22.0), and *p*-values <0.05 were considered statistically significant.

## Results

### Group characteristics

Eighteen adolescents with AIS were included; one was considered as an outlier for morphologic vestibular parameters and was excluded from the study.

Table 1. Group characteristics.

	Scoliosis	Control	p-value
Number	17	9	
Sex Ratio (M/F)	4/13	3/6	0.60
Age +/- SD (year)	15.47 (+/- 1.84)	16.7 (+/- 1.5)	0.28
Cobb angle (°) mean +/- SD [min-max]	26.7 +/-8.3 [15–40]	NA	
Dorsal scoliosis	8	NA	
Lumbar scoliosis	5	NA	
Thoracolumbar scoliosis	4	NA	
Right scoliosis	8	NA	
Left scoliosis	6	NA	
Right and left	3	NA	

doi:10.1371/journal.pone.0131120.t001

Further analyses were thus realized with a scoliosis group including 17 patients, and a control group including 9 participants. Both groups were similar in age and sex ratio and were free from otologic disease according to the ENT specialist (Table 1).

### Orientation of the lateral SCC: The left lateral SCC is more vertical in scoliosis

Both lateral SCCs formed a smaller angle together in the scoliosis group as measured by the IA ( $p = 0.004$ ) with a large difference compared to control ( $r = 0.46$ ) (Table 2). Consequently, an IA of less than or equal to  $170^\circ$  was 100% specific for scoliosis, with a sensitivity of 59% (Fig 4).

The difference in orientation mostly concerned the left lateral SCC, which is closer to vertical as illustrated by a much smaller VLFL ( $p < 0.001$ ;  $r = 0.6$ ).

This vertical orientation of the left lateral SCC is strongly correlated with the position of the vestibule in the scoliosis group ( $r = -0.6$ ;  $p = 0.02$ ). The more vertical the left SCC orientation is (i.e. smaller VLFL), the further the left vestibule is from the midline (i.e. longer LDL, ADL, PDL).

Conversely, the right lateral SCC showed no significant difference between the two groups. This asymmetry between VLFR and VLFL was mostly left sided (58%) in the scoliosis group ( $VLFR - VLFL > 0$ ), but right sided (75%) in the control group ( $VLFR - VLFL < 0$ ) ( $p = 0.15$ ).

Table 2. Left lateral SCC is more vertical in scoliosis.

Orientation of Lateral Semicircular Canal	Scoliosis(1)	Control (1)	Significance(p)	t(df) or U (2)	Effect size « r »
AI	168.9 +/-7.0	175.1 +/-2.8	0.004**	t(23) = -3.25	0.46
VLFR	85 +/-5.4	85.3 +/-3.9	0.86	t(22) = -0.18	0.03
VLFL	83.9 +/-3.5	88.6 +/-1.9	<0.001**	t(23) = -4.4	0.60
Diff VLFR-VLFL	1.15 +/-6.0	-2.3 +/-3.3	0.15	t(23) = 1.5	0.30
AbsolDiffVLFR-VLFL	3.0 (13.6)	3.0 (11.8)	0.57	U = 58.0	0.11
VLSR	78.4 +/-6.6	77.7 +/-6.7	0.81	t(22) = -0.24	0.06
VLSL	79.0 +/-7.4	76.7 +/-5.3	0.47	t(21) = -0.73	0.16

(1) Mean (in degrees) +/- SD if T Test; or Median (in mm) (Mean Rank) if Mann Whitney U test.

(2) t value and degrees of freedom (df) if T Test; or U value if Mann Whitney U test.

\*\*Significance < 0.01.

doi:10.1371/journal.pone.0131120.t002



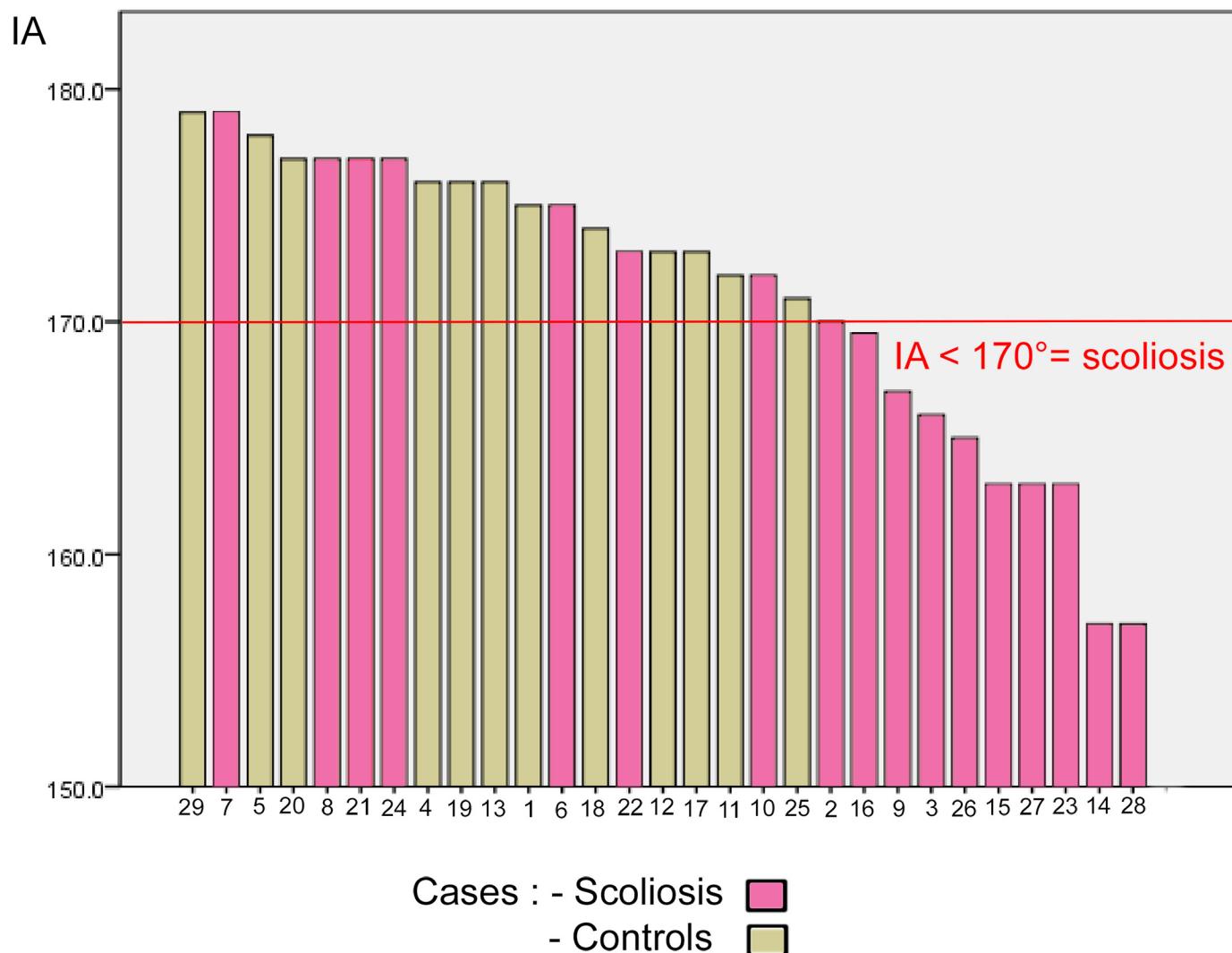


**Fig 4. Intercanal Angle (IA) in scoliosis and controls.** An IA less than or equal to 170° is 100% specific for scoliosis.

doi:10.1371/journal.pone.0131120.g004

Contrary to the frontal plane, analysis in the parasagittal plane showed no significant differences between the two groups (Table 2).

### Position of the SCC: the left canals are further from the midline in scoliosis

The left lateral SCC and the left posterior SCC were significantly further from the midline in scoliosis compared to controls. The left anterior SCC was also further from the midline in scoliosis, but the difference compared to controls was smaller and non significant (Table 3). Of note, the position of the left lateral SCC is strongly correlated with the vertical orientation of this canal (i.e VLFL). The further the canal was from the midline, the more vertical it became (Table 4). However, the right side exhibited neither significant differences between scoliosis and control ( $r < 0.11$ ,  $p > 0.63$ ) nor correlation between SCC position and lateral canal orientation (Tables 3 and 4).

**Table 3. Left lateral SCC and posterior SCC are further from the midline in scoliosis.**

Distances of Semicircular Canal vertex from the Midline	Scoliosis (1)	Control (1)	Significance(p)	T(df) or U (2)	Effect size « r »
LDR	42.9 +/-1.8	42.6+/-1.3	0.63	t(20) = -0.49	0.11
LDL	43.9+/-1.8	42.3+/-3.9	0.01*	t(20) = -2.16	0.44
Diff LDR-LDL	-0.93+/-1.5	0.29+/-1.1	0.08	t(20) = -1.88	0.39
[Diff LDR-LDL]	1.0 (12.3)	1.0 (9.9)	0.40	U = 41.0	0.18
ADR	39.0+/-0.5	40.0+/-1.5	0.97	U = 52.0	0.01
ADL	40.2+/-2.0	39.3+/-1.1	0.19	t(20) = 1.12	0.24
Diff ADR-ADL	-0.13+/-1.4	0.42+/-3.3	0.43	t(20) = -0.80	0.18
[Diff ADR-ADL]	1.0 (10.6)	2.0 (13.4)	0.30	U = 39.0	0.22
PDR	40.4+/-1.7	40.2+/-1.6	0.74	t(20) = 0.30	0.08
PDL	41.0 (13.3)	40.0 (7.7)	0.05*	U = 26.0	0.41
Diff PDR-PDL	-0.8+/-1.6	0.29+/-1.7	0.18	t(20) = -1.40	0.30
[Diff PDR-PDL]	1.0 (11.7)	2.0 (11.1)	0.82	U = 49.0	0.05

(1) Mean (in mm) +/- SD if T Test; or Median (in mm) (Mean Rank) if Mann Whitney U test.

(2) t value and degrees of freedom (df) if T Test; or U value if Mann Whitney U test.

\*significant results with  $p$ -value < 0.05.

doi:10.1371/journal.pone.0131120.t003

## Function of the lateral SCC

Two adolescents with scoliosis exhibited a spontaneous nystagmus. The first was a permanent horizontal left nystagmus associated with a dorsal right-lumbar left scoliosis. This patient was excluded from the caloric test analysis because the spontaneous and caloric nystagmus were difficult to separate. The second patient exhibited an intermittent positional right nystagmus associated with an abnormal right canal paresis (35%) and was included in the group analysis. In the scoliosis group, vestibular excitability was lower but the difference was small ( $r = 0.238$ ) and non significant ( $p = 0.25$ ) compared to controls. The directional preponderance was abnormal ( $< 2^\circ/\text{s}$ ) in half of the participants in both groups ( $p = 0.41$ ).

Canal paresis was higher in the scoliosis group (mean = 18.25% +/- 16.37) compared to controls (mean = 10.33% +/- 5.87), but the difference was not significant according to the Mann Whitney test ( $p = 0.52$ ). Six of the 16 adolescents with scoliosis had abnormal ( $> 15\%$ ) canal paresis compared to only 1 in the 9 controls ( $X(1) = 1.99$ ;  $p = 0.158$ ) (Table 5).

**Table 4. In scoliosis the orientation of the left lateral SCC is correlated with its position and other left SCC positions.**

Parameter1	Parameter2	Coefficient of correlation	p-value
VLFL	LDL	-0.60	0.02*
	PDL	-0.60	0.02*
	ADL	-0.50	0.04*
VLFR	LDR	-0.12	0.67
	PDR	0.22	0.44
	ADR	0.25	0.37
IA	LDL	-0.26	0.35
	LDR	-0.38	0.16

\*Significant results with  $p$ -value < 0.05.

doi:10.1371/journal.pone.0131120.t004

**Table 5. Lateral SCC function.**

Caloric	Scoliosis	Control	Significance(p)	T(df) or U (1)	Effect size « r »
Vestibular excitability (°/s)	33.95+/-15.6	41.77+/-15.4	0.25	T(23) = -1.17	0.238
Directional Preponderance(°/s)	1.953+/-1.8	2.027+/-2.03	0.26	T(23) = -1.16	0.235
Directional preponderance >2°/s (n/total)	8/15	4/8	0.445		
Canal paresis mean(%)	18.25 +/-4.09	11.6 +/-1.67			
Canal paresis median (%)	13.2	11.2	0.52	U = 53.5	0.13
Canal paresis >15% (n/total)	6/16	1/9	0.218		

(1) t value and degrees of freedom (df) if T Test; or U value if Mann Whitney U test; or  $\chi$  value (degrees of freedom) if Chi square test.

doi:10.1371/journal.pone.0131120.t005

## Analysis within the scoliosis group

**Analysis of location of the scoliosis.** The IA was significantly different for the location of the scoliosis group. In particular, thoracolumbar scoliosis ( $n = 4$ ) showed a smaller IA with a mean difference of 11.5° scoliosis compared to lumbar scoliosis ( $n = 5$ ) ( $p = 0.033$ ).

Thoracolumbar scoliosis also showed a more marked asymmetry in the location of lateral SCCs with a right canal located more laterally than the left compare with dorsal scoliosis ( $p < 0.05$ ) or lumbar scoliosis ( $p < 0.03$ ).

Two-way ANOVA combining location and side of scoliosis showed non significant main effects in morphologic or functional vestibular parameters.

**Analysis of side of the scoliosis.** Right and left scoliosis were comparable for morphologic and functional vestibular parameters ( $p > 0.05$ ).

We found no significant association between the side of scoliosis and the side of asymmetries for the position, orientation, or function of the lateral SCC.

**Correlation of the Cobb angle with morphologic or functional vestibular parameters.** No significant correlation was found between the Cobb angle and any morphological or functional parameters of the lateral SCC. ( $p > 0.05$ ).

We found no correlation between age and the Cobb angle nor with age and morphologic parameters of the lateral SCC.

## Relation between vestibular morphology and vestibular function

Scoliosis and control participants with abnormal canal paresis (i.e. >15°) exhibited more vertical lateral SCC as shown by the smaller IA, VLFR, and VLFL ( $r > 0.4$ ,  $p < 0.05$ ) (Table 6). Canal paresis (for both groups) correlated with the IA, the VLFR, the VLFL, the LDL, and the ADL (Table 7). Nevertheless, no significant difference was demonstrated for these parameters linked

**Table 6. Abnormal canal paresis is associated with more vertical lateral SCC.**

Vestibular Morphology	Paresis <15% (1)	Paresis >15% (1)	Significance (p-value)	T(df) (2)	Effect size « r »
IA	173.06+/-5.0	165.57+/-7.8	0.01 *	T(22) = 2.83	0.52
VLFR	86.35+/-4.1	82.29+/-4.7	0.046*	T(22) = 2.11	0.41
VLFL	86.71+/-3.1	83.29+/-3.5	0.026*	T(22) = 2.39	0.45

(1) Mean +/- SD in Scoliosis and control groups.

(2) t value (degrees of freedom) for T Test.

\*Significant results with  $p$ -value < 0.05.

doi:10.1371/journal.pone.0131120.t006

**Table 7. Scoliosis and controls: Canal paresis is correlated with lateral SCC morphology.**

Canal paresis correlation with	Coefficient correlation <i>r</i>	Significance <i>p</i> -value
AI	-0.60	0.001**
VLFR	-0.433	0.02*
VLFL	-0.422	0.04*
VLSR	0.193	0.38
VLSL	0.22	0.33
LDR	0.343	0.1
LDL	0.42	0.04*
PDR	0.178	0.40
PDL	0.244	0.25
ADR	0.002	0.99
ADL	0.507	0.01*

Pearson correlation for parametric distribution, or Spearman Rank.

\*Significant results with *p*-value < 0.05.

\*\* Significant results with *p*-value<0.01.

doi:10.1371/journal.pone.0131120.t007

to the scoliosis group ( $p>0.75$ ) or the side of abnormal canal paresis ( $p>0.056$ ) (two-way ANOVA).

## Discussion

This study shows that adolescents with idiopathic scoliosis present an inner ear asymmetry characterized by a left semicircular canal which is more vertically oriented compared to a control group. This view is in accordance with the results of Shi et al. who demonstrated, in girls with left scoliosis, a shorter distance between the centers of the lateral SCC and the superior SCC on the left side [52]. Our study includes right and left scoliosis with no significant differences between both sides, but as in Shi et al. study the labyrinth abnormality was only observed in the left side [52]. The concordant abnormality described by Shi et al. and in our study implies a malformation of the labyrinth itself. Additionally, our study showed that the left labyrinth in adolescents with scoliosis presents a lateral and a posterior canal located more laterally compared to a control group. This could result from a malformation either of the labyrinth itself, or of the entire petrous bone. Enlarged left skull vaults have been seen in scoliosis [10], but no information about the petrous bone is available at the present time. Of note, the orientation of the lateral SCC is strongly correlated with the position of the 3 SCCs, indicating that both are due to a labyrinth malformation or that the left labyrinth malformation is associated with a malformed left petrous bone.

In either case, these asymmetries of the labyrinth and the skull complement other published findings of asymmetries in the scoliotic skeleton including the pelvis, the mandible, and the ribs [7–10]. These asymmetries support a biomechanical theory whereby one anomaly could mechanically provoke other deformities [10,27,53–56] [10,27,53–55]. However, no link between these asymmetries is demonstrated and they could be independent or due to a common cause.

According to Cox et al., the orientation of the lateral SCC (related to midsagittal or horizontal planes) does not change during embryogenesis [57], and the shape and orientation of the labyrinth is normally fixed early because of prenatal ossification [36–43]. This particularity of the bone of the labyrinth is explained by a high expression of *opg* gene, associated with a low expression of *bmp3* gene [58] responsible for an inhibition of bone remodeling and resulting in

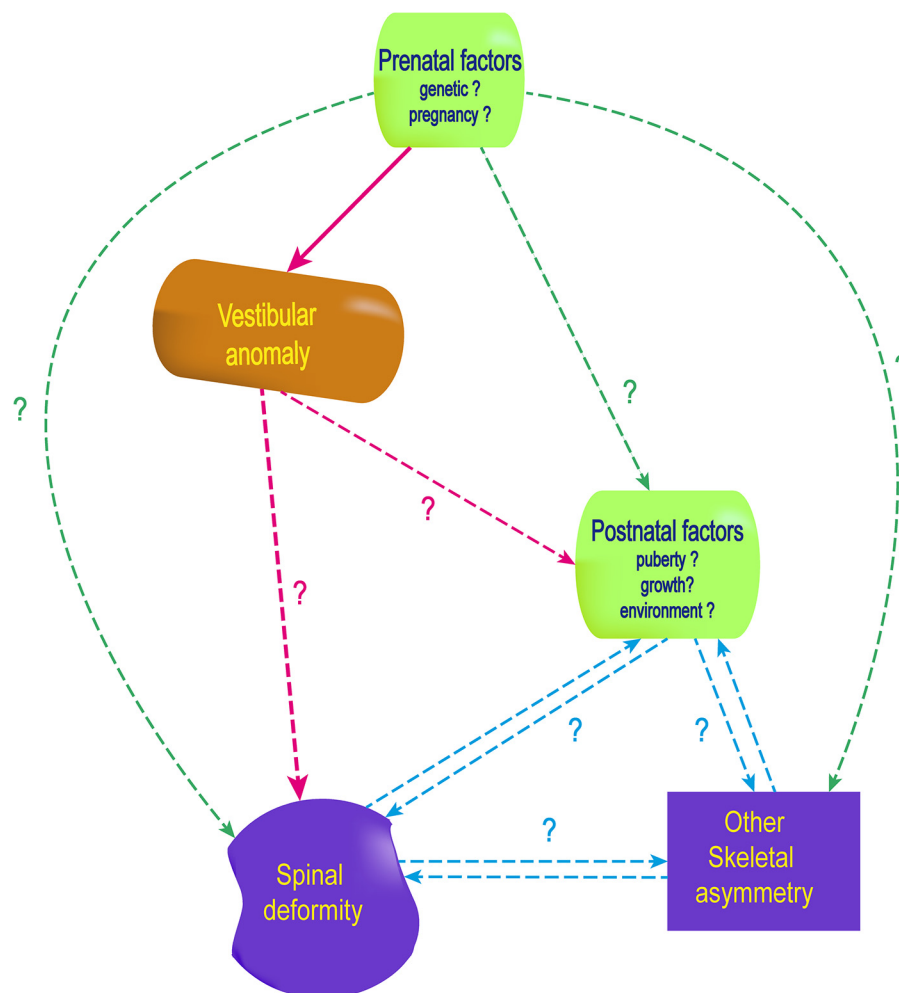


**Fig 5. Early anomalies of the vestibular system in AIS pathogenesis and consequences in adolescent idiopathic scoliosis pathogenesis.** The pink dash arrows represent the hypothesis that a vestibular anomaly may be the cause of later anomalies, including spinal deformity. Different mechanisms supporting this hypothesis are illustrated in Fig 6.

doi:10.1371/journal.pone.0131120.g005

the densest bone in the human body [38,59–63]. Consequently, anomalies observed in an adolescent's labyrinth, would already have been present at birth and probably before the 35<sup>th</sup> week *in utero*. Thus, the labyrinth asymmetry would not be the consequence of the spine deformity but rather its cause. If this is not the case, both abnormalities would come from a common cause or each from a separate origin (Fig 5).

Among these three hypotheses, animal models argue for a vestibular impairment causing the spine deformity. Indeed experimental vestibular lesion in animals induces scoliosis [34,35]. Studies in *Xenopus* underline that vestibular impairment needs to be early (before metamorphosis) to induce osseous deformation, which is in accordance with our hypothesis of early bony labyrinth anomalies in AIS [35].

Our study found abnormal canal paresis in more than one-third of the AIS group. Results of functional tests show substantial variation within the scoliosis group which may decrease the statistical significance when compared to the control group. We noted a correlation between a deficit in the caloric test and the angle of the lateral SCC in the frontal plane (i.e. IA, VLFL, and

VLFR). This could suggest that the verticalization of the lateral SCC either reduces the conduction of the water temperature during the test, or is associated with a functional impairment.

In a previous study with caloric testing in AIS, Sahlstrand and al. found a significantly lower vestibular response located on the side of the spine concavity in AIS [33]. But they found no significant difference in a control group [33], and neither did Wiener et al. [14]. Additionally, Sahlstrand and al. observed oculomotor anomalies in more than half of their AIS group that were either spontaneous (15%) or positional (36%) nystagmus (without describing the orientation). Spontaneous nystagmus can signify a SCC impairment, and in our study the two horizontal nystagmus more specifically indicated a lateral SCC. Positional nystagmus is interpreted by Sahlstrand et al. to originate from the brainstem [33].

In addition to the lateral SCC, the otolith function could also be impaired in AIS since the utricle is known to be roughly parallel to the lateral SCC [64]. The function of otolith sensors (i.e. utricle and saccule) have been studied using off-vertical-axis rotation in patients with scoliosis. Sixty-seven percent exhibited a significantly greater value of directional preponderance, arguing for an impairment of the vestibulospinal function [14].

Additionally, AIS patient show worse sway (relative to controls) when vestibular inputs are the only available [15]. Taken together these studies suggest a vestibular system involved in AIS. Yet anomalies of the vestibular organ alone are not sufficient to explain long-term postural impairment leading to spinal deformity.

Complete vestibular asymmetry (e.g. unilateral labyrinthectomy or vestibular neurectomy) results in postural symptoms which quickly disappear due to central compensation [65,66]. In addition, in normal human, the brain manages physiological asymmetry because of vestibular predominance in the side of handedness [67,68].

AIS symptoms could thus result from vestibular organ abnormalities associated with brain impairments which can be detected by MRI studies. White matter in the corpus callosum and left corticothalamic tract shows changes [30]. Cortical areas, including vestibular cortices, are thinner and there are changes in the cortical network [31,69,70]. The ventral brainstem is also asymmetric and the cerebellum is thicker in the right lobules VIIIA, VIIIB, and the bilateral lobules X [32,71]. Of note, the cerebellum (including lobule VIII) is connected to the vestibular system either directly from the vestibular organ or through the vestibular nuclei complex [72–78] (Fig 6). Moreover, the cerebellum is particularly rich in melatonin receptor, a hormone suspected of acting in scoliosis pathogenesis [12,55,79]. Melatonin reciprocally interacts with the vestibular system by influencing the firing of the medial vestibular nuclei [80], the vestibul sympathetic system [81], and balance [82] (Fig 6).

Anomalies of the central nervous system in AIS may constitute an adaptation to compensate for the instability induced by the spine deformity [32]. They also could result from early abnormal vestibular input occurring at a critical period for the central nervous system. The lack of appropriate inputs during critical periods induce permanent brain abnormalities, as demonstrated for the visual [83], auditory [84] and tactile [85] sensory systems. Critical periods are demonstrated for the vestibular system [86,87] and for multisensory integration as well. Therefore, brain anomalies and multisensory impairments demonstrated in AIS could result from early vestibular abnormalities appearing before the critical period [15,16,88,89]. This point is reinforced by animal models where scoliosis appears only if vestibular lesion is early enough [35].

Finally, in addition to early modification of the central nervous system and the vestibulospinal pathway, the vestibular system could also contribute to spine deformity by influencing the neuroendocrine or the vestibul sympathetic system (Fig 6). In fact, the lateral vestibular nuclei and the vestibular cortex (e.g. the insula) project out to the lateral hypothalamus which is rich in leptin receptors [90–93]. Leptin is one of the main hormones suspected of being involved in



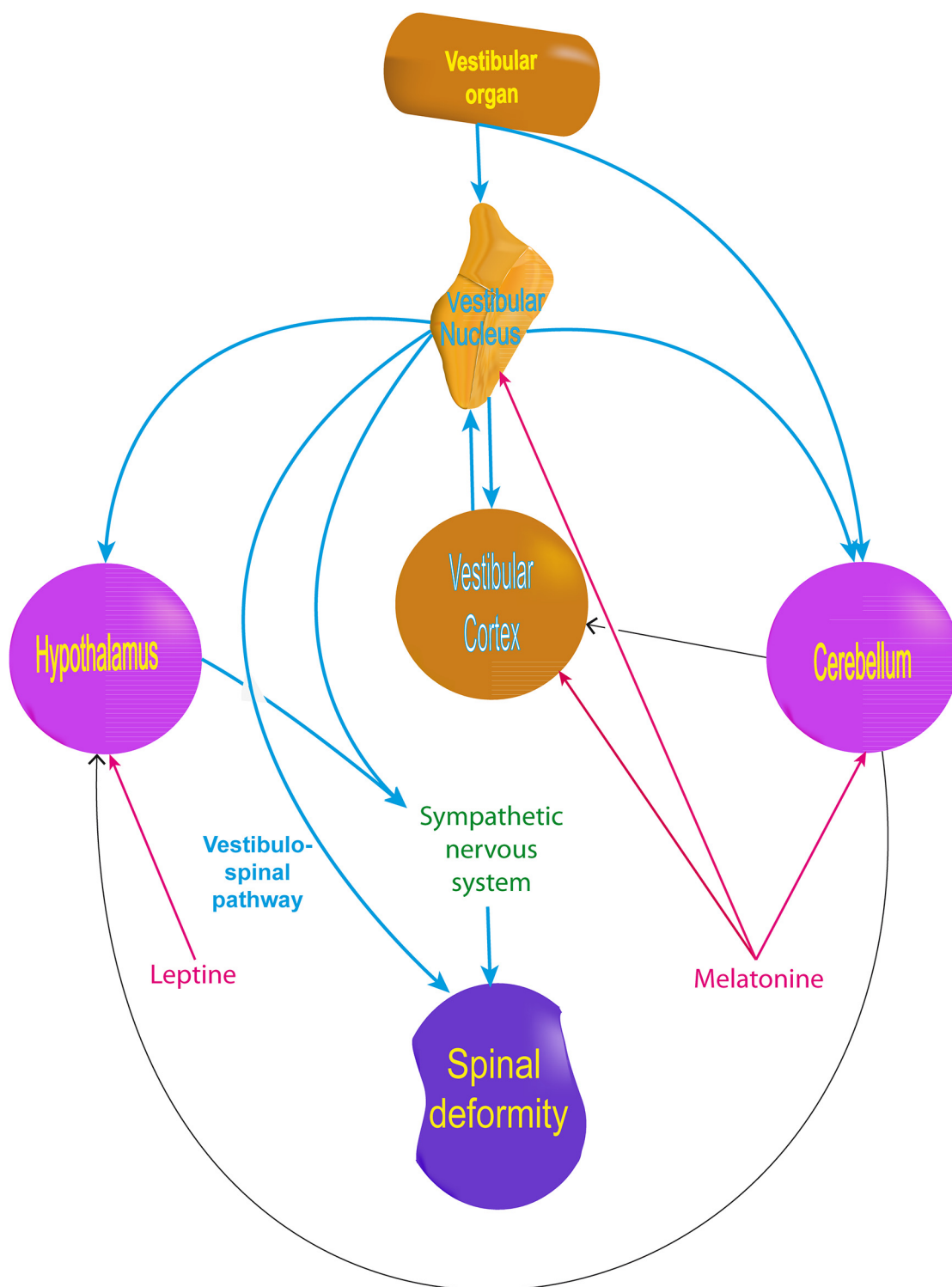


**Fig 6. Influence of the vestibular system on key elements involved in AIS pathogenesis theories, including hormonal and neurosensory theories.**

doi:10.1371/journal.pone.0131120.g006

scoliosis [27]. The lateral hypothalamus, the cerebellum, and the rostro-ventro-lateral medullary structure also influence the vestibulosympathetic system [94–96] which regulates bone

remodeling [97,98]. Therefore, the vestibular sympathetic system may contribute to bone deformity and to the bone demineralization demonstrated in adolescent scoliosis [99–102].

Altogether, these results are in accordance with: 1) in the biomechanical theory of AIS, early asymmetry exists before the spine deformity and may therefore be its cause rather than its consequence; 2) in the endocrine theory, the vestibular anomalies could interact with hormones early before puberty; 3) in the neurosensory theory, vestibular impairment may start early enough to influence brain maturation and might precede the biomechanical or hormonal phenomena.

The multiple consequences of an early vestibular impairment, including some compensatory mechanisms, may explain why the lateral SCC parameters are not directly correlated with the Cobb angle. Another reason may be that scoliosis is a dynamic process and etiologic factor(s) may correlate to the progression of the process rather than the degree of spine deformity in one measurement. Furthermore, the mild spine deformities of our participants (Cobb's angle  $< 40^\circ$ ) may decrease the chance of demonstrating statistical correlation. The influence of these last two factors was demonstrated in sway in AIS where participants exhibit more impairment in case of deformities  $> 40^\circ$  or progression  $> 10^\circ/\text{year}$ . [103]

Additionally, other factors (e.g. sex, body mass index, internal organ asymmetry) may also explain the lack of correlation, for example between the left lateral SCC anomalies and the side of the scoliosis [27,104–107]. The involvement of late factors appearing during childhood or puberty is also likely to explain why the spine deformity appears only in adolescence despite the early vestibular anomaly. Lastly, vestibular anomaly may also act as an onset factor of scoliosis without further role in progression.[108]

Finally our results lead to another question: What is the origin of the lateral SCC anomaly? The estimate of early occurrence of the malformation focuses the answer on genetic factors and/or environmental factors during pregnancy. This underscores that lateral SCC malformation and spine deformity could also be independent from each other but induced by a common cause. One hypothesis of common causes could be genes involved in growth acceleration occurring during SCC embryogenesis [42] and puberty.

## Conclusion

We have used the labyrinth of adolescents as a “living fossil” to explore the chronology of AIS and to show that anomalies of the vestibular system start before birth. As the earliest anomaly demonstrated so far, the vestibule may be the cause of the spinal deformity. If not, both anomalies might still result from a common cause which appears before birth according to the timing of the vestibular malformation. In either case, findings encourage the search during pregnancy for causative environmental factors which could lead to prenatal preventive treatment. Moreover, a simple MRI measurement of the lateral SCC, as demonstrated here, could be used to predict AIS and initiate preventive treatment during childhood. However, the best treatments will certainly need a complete understanding of AIS chronology which requires multiple landmarks. The lateral semicircular canal constitutes a first milestone which can now open the road to longitudinal studies.

## Supporting Information

**S1 Table. Data set of each participant.**  
(XLSX)

## Acknowledgments

We thank Dr. Vincent Patron, Dr. Stéphane Besnard and two anonymous reviewers for their comments on the manuscript.

## Author Contributions

Conceived and designed the experiments: PD GQ JFM M. Hitier M. Hamon. Performed the experiments: JL JFM M. Hamon MAT SM. Analyzed the data: JL M. Hitier. Contributed reagents/materials/analysis tools: SM. Wrote the paper: M. Hitier PD.

## References

1. Kane WJ. Scoliosis prevalence: a call for a statement of terms. *Clin Orthop*. 1977; 126: 43–46. PMID: [598138](#)
2. Reamy BV, Slakey JB. Adolescent idiopathic scoliosis: review and current concepts. *Am Fam Physician*. 2001; 64: 111–116. PMID: [11456428](#)
3. Weinstein SL, Dolan LA, Cheng JCY, Danielsson A, Morcuende JA. Adolescent idiopathic scoliosis. *The Lancet*. 2008; 371: 1527–1537.
4. Altat F, Gibson A, Dannawi Z, Noordeen H. Adolescent idiopathic scoliosis. *BMJ*. 2013; 346: f2508. doi: [10.1136/bmj.f2508](#) PMID: [23633006](#)
5. Asher MA, Burton DC. Adolescent idiopathic scoliosis: natural history and long term treatment effects. *Scoliosis*. 2006; 1: 2. doi: [10.1186/1748-7161-1-2](#) PMID: [16759428](#)
6. Schlösser TPC, van der Heijden GJMG, Versteeg AL, Castelein RM. How “Idiopathic” Is Adolescent Idiopathic Scoliosis? A Systematic Review on Associated Abnormalities. *PLoS ONE*. 2014; 9: e97461. doi: [10.1371/journal.pone.0097461](#) PMID: [24820478](#)
7. Burwell RG, Aujla RK, Freeman BJC, Dangerfield PH, Cole AA, Kirby AS, et al. Patterns of extra-spinal left-right skeletal asymmetries in adolescent girls with lower spine scoliosis: relative lengthening of the ilium on the curve concavity & of right lower limb segments. *Stud Health Technol Inform*. 2006; 123: 57–65. PMID: [17108404](#)
8. Normelli H, Sevastik J, Akrivos J. The length and ash weight of the ribs of normal and scoliotic persons. *Spine*. 1985; 10: 590–592. PMID: [4081873](#)
9. Burwell RG, Freeman BJC, Dangerfield PH, Aujla RK, Cole AA, Kirby AS, et al. Left-right upper arm length asymmetry associated with apical vertebral rotation in subjects with thoracic scoliosis: anomaly of bilateral symmetry affecting vertebral, costal and upper arm physes? *Stud Health Technol Inform*. 2006; 123: 66–71. PMID: [17108405](#)
10. Shi L, Heng PA, Wong T-T, Chu WCW, Yeung BHY, Cheng JCY. Morphometric analysis for pathological abnormality detection in the skull vaults of adolescent idiopathic scoliosis girls. *Med Image Comput Comput Assist Interv*. 2006; 9: 175–182. PMID: [17354888](#)
11. Qiu Y, Sun X, Qiu X, Li W, Zhu Z, Zhu F, et al. Decreased circulating leptin level and its association with body and bone mass in girls with adolescent idiopathic scoliosis. *Spine*. 2007; 32: 2703–2710. doi: [10.1097/BRS.0b013e31815a59e5](#) PMID: [18007248](#)
12. Moreau A, Forget S, Azeddine B, Angeloni D, Frascini F, Labelle H, et al. Melatonin signaling dysfunction in adolescent idiopathic scoliosis. *Spine*. 2004; 29: 1772–1781. PMID: [15303021](#)
13. Girardo M, Bettini N, Dema E, Cervellati S. The role of melatonin in the pathogenesis of adolescent idiopathic scoliosis (AIS). *Eur Spine J*. 2011; 20 Suppl 1: S68–74. doi: [10.1007/s00586-011-1750-5](#) PMID: [21416282](#)
14. Wiener-Vacher SR, Mazda K. Asymmetric otolith vestibulo-ocular responses in children with idiopathic scoliosis. *J Pediatr*. 1998; 132: 1028–1032. PMID: [9627598](#)
15. Simoneau M, Lamothe V, Hutin É, Mercier P, Teasdale N, Blouin J. Evidence for cognitive vestibular integration impairment in idiopathic scoliosis patients. *BMC Neurosci*. 2009; 10: 102. doi: [10.1186/1471-2202-10-102](#) PMID: [19706173](#)
16. Assaiante C, Mallau S, Jouve J-L, Bollini G, Vaugoyeau M. Do Adolescent Idiopathic Scoliosis (AIS) Neglect Proprioceptive Information in Sensory Integration of Postural Control? *PLoS ONE*. 2012; 7: e40646. doi: [10.1371/journal.pone.0040646](#) PMID: [22815779](#)
17. Simoneau M, Mercier P, Blouin J, Allard P, Teasdale N. Altered sensory-weighting mechanisms is observed in adolescents with idiopathic scoliosis. *BMC Neurosci*. 2006; 7: 68. doi: [10.1186/1471-2202-7-68](#) PMID: [17052338](#)

18. Takahashi Y, Kou I, Takahashi A, Johnson TA, Kono K, Kawakami N, et al. A genome-wide association study identifies common variants near LBX1 associated with adolescent idiopathic scoliosis. *Nat Genet.* 2011; 43: 1237–1240. doi: [10.1038/ng.974](https://doi.org/10.1038/ng.974) PMID: [22019779](https://pubmed.ncbi.nlm.nih.gov/22019779/)
19. Kou I, Takahashi Y, Johnson TA, Takahashi A, Guo L, Dai J, et al. Genetic variants in GPR126 are associated with adolescent idiopathic scoliosis. *Nat Genet.* 2013; 45: 676–679. doi: [10.1038/ng.2639](https://doi.org/10.1038/ng.2639) PMID: [23666238](https://pubmed.ncbi.nlm.nih.gov/23666238/)
20. Londono D, Kou I, Johnson TA, Sharma S, Ogura Y, Tsunoda T, et al. A meta-analysis identifies adolescent idiopathic scoliosis association with LBX1 locus in multiple ethnic groups. *J Med Genet.* 2014; 51: 401–406. doi: [10.1136/jmedgenet-2013-102067](https://doi.org/10.1136/jmedgenet-2013-102067) PMID: [24721834](https://pubmed.ncbi.nlm.nih.gov/24721834/)
21. Chettier R, Nelson L, Ogilvie JW, Albertsen HM, Ward K. Haplotypes at LBX1 Have Distinct Inheritance Patterns with Opposite Effects in Adolescent Idiopathic Scoliosis. *PloS One.* 2015; 10: e0117708. doi: [10.1371/journal.pone.0117708](https://doi.org/10.1371/journal.pone.0117708) PMID: [25675428](https://pubmed.ncbi.nlm.nih.gov/25675428/)
22. Sharma S, Londono D, Eckalbar WL, Gao X, Zhang D, Mauldin K, et al. A PAX1 enhancer locus is associated with susceptibility to idiopathic scoliosis in females. *Nat Commun.* 2015; 6: 6452. doi: [10.1038/ncomms7452](https://doi.org/10.1038/ncomms7452) PMID: [25784220](https://pubmed.ncbi.nlm.nih.gov/25784220/)
23. Miyake A, Kou I, Takahashi Y, Johnson TA, Ogura Y, Dai J, et al. Identification of a Susceptibility Locus for Severe Adolescent Idiopathic Scoliosis on Chromosome 17q24.3. *PLoS ONE.* 2013; 8: e72802. doi: [10.1371/journal.pone.0072802](https://doi.org/10.1371/journal.pone.0072802) PMID: [24023777](https://pubmed.ncbi.nlm.nih.gov/24023777/)
24. Worthington V, Shambaugh P. Nutrition as an environmental factor in the etiology of idiopathic scoliosis. *J Manipulative Physiol Ther.* 1993; 16: 169. PMID: [8492060](https://pubmed.ncbi.nlm.nih.gov/8492060/)
25. De George FV, Fisher RL. Idiopathic scoliosis: genetic and environmental aspects. *J Med Genet.* 1967; 4: 251. PMID: [6082901](https://pubmed.ncbi.nlm.nih.gov/6082901/)
26. Kouwenhoven J-WM, Castelein RM. The pathogenesis of adolescent idiopathic scoliosis: review of the literature. *Spine.* 2008; 33: 2898–2908. doi: [10.1097/BRS.0b013e3181891751](https://doi.org/10.1097/BRS.0b013e3181891751) PMID: [19092622](https://pubmed.ncbi.nlm.nih.gov/19092622/)
27. Burwell RG, Aujla RK, Grevitt MP, Dangerfield PH, Moulton A, Randell TL, et al. Pathogenesis of adolescent idiopathic scoliosis in girls—a double neuro-osseous theory involving disharmony between two nervous systems, somatic and autonomic expressed in the spine and trunk: possible dependency on sympathetic nervous system and hormones with implications for medical therapy. *Scoliosis.* 2009; 4: 24. doi: [10.1186/1748-7161-4-24](https://doi.org/10.1186/1748-7161-4-24) PMID: [19878575](https://pubmed.ncbi.nlm.nih.gov/19878575/)
28. Wang WJ, Yeung HY, Chu WC-W, Tang NL-S, Lee KM, Qiu Y, et al. Top theories for the etiopathogenesis of adolescent idiopathic scoliosis. *J Pediatr Orthop.* 2011; 31: S14–27. doi: [10.1097/BPO.0b013e3181f73c12](https://doi.org/10.1097/BPO.0b013e3181f73c12) PMID: [21173615](https://pubmed.ncbi.nlm.nih.gov/21173615/)
29. Lowe TG, Edgar M, Margulies JY, Miller NH, Raso VJ, Reinker KA, et al. Etiology of Idiopathic Scoliosis: Current Trends in Research\*. *J Bone Jt Surg.* 2000; 82: 1157–1157.
30. Shi L, Wang D, Chu WCW, Burwell RG, Freeman BJC, Heng PA, et al. Volume-based morphometry of brain MR images in adolescent idiopathic scoliosis and healthy control subjects. *AJNR Am J Neuroradiol.* 2009; 30: 1302–1307. doi: [10.3174/ajnr.A1577](https://doi.org/10.3174/ajnr.A1577) PMID: [19386729](https://pubmed.ncbi.nlm.nih.gov/19386729/)
31. Wang D, Shi L, Chu WC, Burwell RG, Cheng JC, Ahuja AT. Abnormal cerebral cortical thinning pattern in adolescent girls with idiopathic scoliosis. *Neuroimage.* 2012; 59: 935–942. doi: [10.1016/j.neuroimage.2011.07.097](https://doi.org/10.1016/j.neuroimage.2011.07.097) PMID: [21872666](https://pubmed.ncbi.nlm.nih.gov/21872666/)
32. Shi L, Wang D, Hui SCN, Tong MCF, Cheng JCY, Chu WCW. Volumetric changes in cerebellar regions in adolescent idiopathic scoliosis compared with healthy controls. *Spine J.* 2013; 13: 1904–1911. doi: [10.1016/j.spinee.2013.06.045](https://doi.org/10.1016/j.spinee.2013.06.045) PMID: [23988458](https://pubmed.ncbi.nlm.nih.gov/23988458/)
33. Sahlstrand T, Petruson B. A Study of Labyrinthine Function in Patients with Adolescent Idiopathic Scoliosis I. An Electro-Nystagmographic Study. *Acta Orthop.* 1979; 50: 759–769.
34. De Waele C, Graf W, Josset P, Vidal PP. A radiological analysis of the postural syndromes following hemilabyrinthectomy and selective canal and otolith lesions in the guinea pig. *Exp Brain Res.* 1989; 77: 166–182. PMID: [2792260](https://pubmed.ncbi.nlm.nih.gov/2792260/)
35. Lambert FM, Malinvaud D, Glaunès J, Bergot C, Straka H, Vidal PP. Vestibular asymmetry as the cause of idiopathic scoliosis: a possible answer from *Xenopus*. *J Neurosci.* 2009; 29: 12477–12483. doi: [10.1523/JNEUROSCI.2583-09.2009](https://doi.org/10.1523/JNEUROSCI.2583-09.2009) PMID: [19812323](https://pubmed.ncbi.nlm.nih.gov/19812323/)
36. Sato T. Vergleichende Untersuchungen über die Bogengänge des Labyrinthes beim neugeborenen und beim erwachsenen Menschen. Wiesbaden: Bergmann; 1902.
37. Bast TH. Ossification of the otic capsule in human fetuses. *Contributions to Embryology.* Washington: Carnegie Institution of Washington; 1930.
38. Bast TH, Anson BJ. The temporal bone and the ear. Springfield, IL: CC Thomas; 1949.
39. Hublin J-J, Spoor F, Braun M, Zonneveld F, Condemi S. A late Neanderthal associated with Upper Palaeolithic artefacts. *Nature.* 1996; 381: 224–226. PMID: [8622762](https://pubmed.ncbi.nlm.nih.gov/8622762/)

40. Spoor F, Esteves F, Tecelão Silva F, Pacheco Dias R. The bony labyrinth of Lagar Velho 1. The Lapedo Child, a Gravettian Human Skeleton from the Abrigo Do Lagar Velho. Zilhao J, Trinkhaus E, Duarte C. Lisbon: Instituto Portugus de Arqueologia; 2002. pp. 287–292.
41. Spoor F, Hublin J-J, Kondo O. The bony labyrinth of the Dederiyeh child. Neanderthal Burials Excavations of the Dederiyeh Cave, Afrin, Syria. Tokyo: The Tokyo University Press; 2002. pp. 215–220.
42. Jeffery N, Spoor F. Prenatal growth and development of the modern human labyrinth. *J Anat.* 2004; 204: 71–92. doi: [10.1111/j.1469-7580.2004.00250.x](https://doi.org/10.1111/j.1469-7580.2004.00250.x) PMID: [15032915](https://pubmed.ncbi.nlm.nih.gov/15032915/)
43. Dahm MC, Shepherd RK, Clark GM. The Postnatal Growth of the Temporal Bone and its Implications for Cochlear Implantation in Children. *Acta Otolaryngol (Stockh).* 2009; 113: 4–39.
44. Curthoys IS. The interpretation of clinical tests of peripheral vestibular function. *The Laryngoscope.* 2012; 122: 1342–1352. doi: [10.1002/lary.23258](https://doi.org/10.1002/lary.23258) PMID: [22460150](https://pubmed.ncbi.nlm.nih.gov/22460150/)
45. Nemzek WR, Brodie HA, Chong BW, Babcock CJ, Hecht ST, Salamat S, et al. Imaging findings of the developing temporal bone in fetal specimens. *AJNR Am J Neuroradiol.* 1996; 17: 1467–1477. PMID: [8883642](https://pubmed.ncbi.nlm.nih.gov/8883642/)
46. Richards BS, Sucato DJ, Konigsberg DE, Ouellet JA. Comparison of reliability between the Lenke and King classification systems for adolescent idiopathic scoliosis using radiographs that were not premeasured. *Spine.* 2003; 28: 1148–1156; discussion 1156–1157. doi: [10.1097/01.BRS.0000067265.52473.C3](https://doi.org/10.1097/01.BRS.0000067265.52473.C3) PMID: [12782983](https://pubmed.ncbi.nlm.nih.gov/12782983/)
47. British Society of Audiology. Recommended procedure. The caloric test. London: BSA; 2010.
48. Hallpike CS. The caloric tests. *J Laryngol Otol.* 1956; 70: 15–28. PMID: [13278645](https://pubmed.ncbi.nlm.nih.gov/13278645/)
49. Jonkees LB, Maas JP, Philipszoon AJ. Clinical nystagmography. A detailed study of electro-nystagmography in 341 patients with vertigo. *Pract Otorhinolaryngol (Basel).* 1962; 24: 65–93.
50. Pietkiewicz P, Pepa R, Sułkowski WJ, Zielińska-Bli niewska H, Olszewski J. Electronystagmography versus videonystagmography in diagnosis of vertigo. *Int J Occup Med Environ Health.* 2012; 25: 59–65. doi: [10.2478/s13382-012-0002-1](https://doi.org/10.2478/s13382-012-0002-1) PMID: [22219058](https://pubmed.ncbi.nlm.nih.gov/22219058/)
51. Hoaglin DC, Iglewicz B. Fine-tuning some resistant rules for outlier labeling. *J Am Stat Assoc.* 1987; 82: 1147–1149.
52. Shi L, Wang D, Chu CW, others. Automatic MRI Segmentation and morphoanatomy of the vestibular system in adolescent idiopathic scoliosis. *Neuroimage.* 2011; 54 Suppl 1: 180–188. doi:10.1016
53. Zhou S, Yan J, Da H, Yang Y, Wang N, Wang W, et al. A correlational study of scoliosis and trunk balance in adult patients with mandibular deviation. *PLoS ONE.* 2013; 8: e59929. doi: [10.1371/journal.pone.0059929](https://doi.org/10.1371/journal.pone.0059929) PMID: [23555836](https://pubmed.ncbi.nlm.nih.gov/23555836/)
54. Dalleau G, Leroyer P, Beaulieu M, Verkindt C, Rivard C-H, Allard P. Pelvis morphology, trunk posture and standing imbalance and their relations to the Cobb angle in moderate and severe untreated AIS. *PLoS ONE.* 2012; 7: e36755. doi: [10.1371/journal.pone.0036755](https://doi.org/10.1371/journal.pone.0036755) PMID: [22792155](https://pubmed.ncbi.nlm.nih.gov/22792155/)
55. Burwell RG, Dangerfield PH, Freeman BJC. Concepts on the pathogenesis of adolescent idiopathic scoliosis. Bone growth and mass, vertebral column, spinal cord, brain, skull, extra-spinal left-right skeletal length asymmetries, disproportions and molecular pathogenesis. *Stud Health Technol Inform.* 2008; 135: 3–52. PMID: [18401079](https://pubmed.ncbi.nlm.nih.gov/18401079/)
56. Kouwenhoven J-WM, Smit TH, van der Veen AJ, Kingma I, van Dieën JH, Castelein RM. Effects of dorsal versus ventral shear loads on the rotational stability of the thoracic spine: a biomechanical porcine and human cadaveric study. *Spine.* 2007; 32: 2545–2550. doi: [10.1097/BRS.0b013e318158cd86](https://doi.org/10.1097/BRS.0b013e318158cd86) PMID: [17978652](https://pubmed.ncbi.nlm.nih.gov/17978652/)
57. Cox PG, Jeffery N. Morphology of the mammalian vestibulo-ocular reflex: The spatial arrangement of the human fetal semicircular canals and extraocular muscles. *J Morphol.* 2007; 268: 878–890. doi: [10.1002/jmor.10559](https://doi.org/10.1002/jmor.10559) PMID: [17659532](https://pubmed.ncbi.nlm.nih.gov/17659532/)
58. Stankovic KM, Adachi O, Tsuji K, Kristiansen AG, Adams JC, Rosen V, et al. Differences in gene expression between the otic capsule and other bones. *Hear Res.* 2010; 265: 83–89. doi: [10.1016/j.heares.2010.02.006](https://doi.org/10.1016/j.heares.2010.02.006) PMID: [20146935](https://pubmed.ncbi.nlm.nih.gov/20146935/)
59. Sørensen MS, Bretlau P, Jørgensen MB. Quantum type bone remodeling in the otic capsule of the pig. *Acta Otolaryngol (Stockh).* 1990; 110: 217–223.
60. Sørensen MS, Bretlau P, Jørgensen MB. Human perilyabyrinthine bone dynamics. A functional approach to temporal bone histology. *Acta Oto-Laryngol Suppl.* 1992; 496: 1–27.
61. Frisch T, Sørensen MS, Overgaard S, Lind M, Bretlau P. Volume-referent bone turnover estimated from the interlabel area fraction after sequential labeling. *Bone.* 1998; 22: 677–682. PMID: [9626408](https://pubmed.ncbi.nlm.nih.gov/9626408/)
62. Frisch T, Overgaard S, Sørensen MS, Bretlau P. Estimation of volume referent bone turnover in the otic capsule after sequential point labeling. *Ann Otol Rhinol Laryngol.* 2000; 109: 33–39. PMID: [10651409](https://pubmed.ncbi.nlm.nih.gov/10651409/)

63. Frisch T Bloch SL Sørensen MS. Prevalence, size and distribution of microdamage in the human otic capsule. *Acta Otolaryngol* (Stockh). 2015; 1–5. doi: [10.3109/00016489.2015.1035400](https://doi.org/10.3109/00016489.2015.1035400)
64. Naganuma H, Tokumasu K, Okamoto M, Hashimoto S, Yamashina S. Three-dimensional analysis of morphological aspects of the human utricular macula. *Ann Otol Rhinol Laryngol*. 2003; 112: 419. PMID: [12784980](https://pubmed.ncbi.nlm.nih.gov/12784980/)
65. Curthoys IS. Vestibular compensation and substitution. *Curr Opin Neurol*. 2000; 13: 27–30. PMID: [10719646](https://pubmed.ncbi.nlm.nih.gov/10719646/)
66. Smith PF, Curthoys IS. Mechanisms of recovery following unilateral labyrinthectomy: a review. *Brain Res Rev*. 1989; 14: 155–180. PMID: [2665890](https://pubmed.ncbi.nlm.nih.gov/2665890/)
67. Dieterich M, Bense S, Lutz S, Drzezga A, Stephan T, Bartenstein P, et al. Dominance for vestibular cortical function in the non-dominant hemisphere. *Cereb Cortex*. 2003; 13: 994–1007. PMID: [12902399](https://pubmed.ncbi.nlm.nih.gov/12902399/)
68. Best C, Lange E, Buchholz H-G, Schreckenberger M, Reuss S, Dieterich M. Left hemispheric dominance of vestibular processing indicates lateralization of cortical functions in rats. *Brain Struct Funct*. 2013; 219: 2141–2158. doi: [10.1007/s00429-013-0628-1](https://doi.org/10.1007/s00429-013-0628-1) PMID: [23979449](https://pubmed.ncbi.nlm.nih.gov/23979449/)
69. Liu T, Chu WCW, Young G, Li K, Yeung BHY, Guo L, et al. MR analysis of regional brain volume in adolescent idiopathic scoliosis: neurological manifestation of a systemic disease. *J Magn Reson Imaging JMRI*. 2008; 27: 732–736. doi: [10.1002/jmri.21321](https://doi.org/10.1002/jmri.21321)
70. Wang D, Shi L, Liu S, Hui SCN, Wang Y, Cheng JCY, et al. Altered Topological Organization of Cortical Network in Adolescent Girls with Idiopathic Scoliosis. *PLoS ONE*. 2013; 8: e83767. doi: [10.1371/journal.pone.0083767](https://doi.org/10.1371/journal.pone.0083767) PMID: [24376742](https://pubmed.ncbi.nlm.nih.gov/24376742/)
71. Geissele AE, Kransdorf MJ, Geyer CA, Jelinek JS, Van Dam BE. Magnetic resonance imaging of the brain stem in adolescent idiopathic scoliosis. *Spine*. 1991; 16: 761–763. PMID: [1925751](https://pubmed.ncbi.nlm.nih.gov/1925751/)
72. Korte GE, Mugnaini E. The cerebellar projection of the vestibular nerve in the cat. *J Comp Neurol*. 1979; 184: 265–277. doi: [10.1002/cne.901840204](https://doi.org/10.1002/cne.901840204) PMID: [762284](https://pubmed.ncbi.nlm.nih.gov/762284/)
73. Angelaki DE, Yakusheva TA, Green AM, Dickman JD, Blazquez PM. Computation of egomotion in the macaque cerebellar vermis. *The Cerebellum*. 2010; 9: 174–182. doi: [10.1007/s12311-009-0147-z](https://doi.org/10.1007/s12311-009-0147-z) PMID: [20012388](https://pubmed.ncbi.nlm.nih.gov/20012388/)
74. Brodal A, Brodal P. Observations on the secondary vestibulocerebellar projections in the macaque monkey. *Exp Brain Res*. 1985; 58: 62–74. PMID: [3987852](https://pubmed.ncbi.nlm.nih.gov/3987852/)
75. Blanks RHI, Precht W, Torigoe Y. Afferent projections to the cerebellar flocculus in the pigmented rat demonstrated by retrograde transport of horseradish peroxidase. *Exp Brain Res*. 1983; 52: 293–306. PMID: [6641889](https://pubmed.ncbi.nlm.nih.gov/6641889/)
76. Carleton SC, Carpenter MB. Distribution of primary vestibular fibers in the brainstem and cerebellum of the monkey. *Brain Res*. 1984; 294: 281–298. PMID: [6200186](https://pubmed.ncbi.nlm.nih.gov/6200186/)
77. Walberg F, Dietrichs E. The interconnection between the vestibular nuclei and the nodulus: a study of reciprocity. *Brain Res*. 1988; 449: 47–53. PMID: [2456133](https://pubmed.ncbi.nlm.nih.gov/2456133/)
78. Kotchabhakdi N, Walberg F. Cerebellar afferent projections from the vestibular nuclei in the cat: an experimental study with the method of retrograde axonal transport of horseradish peroxidase. *Exp Brain Res*. 1978; 31: 591–604. PMID: [350598](https://pubmed.ncbi.nlm.nih.gov/350598/)
79. Mazzucchelli C, Pannacci M, Nonno R, Lucini V, Fraschini F, Michaylov Stankov B. The melatonin receptor in the human brain: cloning experiments and distribution studies. *Mol Brain Res*. 1996; 39: 117–126. PMID: [8804720](https://pubmed.ncbi.nlm.nih.gov/8804720/)
80. Podda MV, Deriu F, Giaconi E, Milia M, Tolu E. Melatonin inhibits rat medial vestibular nucleus neuron activity in vitro. *Neurosci Lett*. 2003; 341: 209–212. PMID: [12697285](https://pubmed.ncbi.nlm.nih.gov/12697285/)
81. Cook JS, Ray CA. Melatonin attenuates the vestibul sympathetic but not vestibulocollic reflexes in humans: selective impairment of the utricles. *J Appl Physiol*. 2010; 109: 1697–1701. doi: [10.1152/japplphysiol.00698.2010](https://doi.org/10.1152/japplphysiol.00698.2010) PMID: [20829497](https://pubmed.ncbi.nlm.nih.gov/20829497/)
82. Fraschini F, Cesarani A, Alpini D, Esposti D, Stankov BM. Melatonin Influences Human Balance. *Neurosignals*. 1999; 8: 111–119. doi: [10.1159/000014578](https://doi.org/10.1159/000014578)
83. Hensch TK. Critical period mechanisms in developing visual cortex. *Curr Top Dev Biol*. 2005; 69: 215–237. PMID: [16243601](https://pubmed.ncbi.nlm.nih.gov/16243601/)
84. Keuroghlian AS, Knudsen EI. Adaptive auditory plasticity in developing and adult animals. *Prog Neurobiol*. 2007; 82: 109–121. PMID: [17493738](https://pubmed.ncbi.nlm.nih.gov/17493738/)
85. Simons DJ, Land PW. Early experience of tactile stimulation influences organization of somatic sensory cortex. *Nature*. 1987; 326: 694–697. doi: [10.1038/326694a0](https://doi.org/10.1038/326694a0) PMID: [3561512](https://pubmed.ncbi.nlm.nih.gov/3561512/)



86. Eugène D, Deforges S, Vibert N, Vidal P-P. Vestibular critical period, maturation of central vestibular neurons, and locomotor control. *Ann N Y Acad Sci*. 2009; 1164: 180–187. doi: [10.1111/j.1749-6632.2008.03727.x](https://doi.org/10.1111/j.1749-6632.2008.03727.x) PMID: [19645897](https://pubmed.ncbi.nlm.nih.gov/19645897/)
87. Moorman SJ, Cordova R, Davies SA. A critical period for functional vestibular development in zebrafish. *Dev Dyn*. 2002; 223: 285–291. PMID: [11836792](https://pubmed.ncbi.nlm.nih.gov/11836792/)
88. Simoneau M, Mercier P, Blouin J, Allard P, Teasdale N. Altered sensory-weighting mechanisms is observed in adolescents with idiopathic scoliosis. *BMC Neurosci*. 2006; 7: 68. PMID: [17052338](https://pubmed.ncbi.nlm.nih.gov/17052338/)
89. Wallace MT, Stein BE. Early experience determines how the senses will interact. *J Neurophysiol*. 2007; 97: 921–926. PMID: [16914616](https://pubmed.ncbi.nlm.nih.gov/16914616/)
90. Risold PY, Thompson RH, Swanson LW. The structural organization of connections between hypothalamus and cerebral cortex. *Brain Res Rev*. 1997; 24: 197–254. doi: [10.1016/S0165-0173\(97\)00007-6](https://doi.org/10.1016/S0165-0173(97)00007-6) PMID: [9385455](https://pubmed.ncbi.nlm.nih.gov/9385455/)
91. Katafuchi T, Puthuraya KP, Yoshimatsu H, Oomura Y. Responses of rat lateral hypothalamic neuron activity to vestibular nuclei stimulation. *Brain Res*. 1987; 400: 62–69. PMID: [3815070](https://pubmed.ncbi.nlm.nih.gov/3815070/)
92. Mercer JG, Hoggard N, Williams LM, Lawrence CB, Hannah LT, Trayhurn P. Localization of leptin receptor mRNA and the long form splice variant (Ob-Rb) in mouse hypothalamus and adjacent brain regions by in situ hybridization. *FEBS Lett*. 1996; 387: 113–116. PMID: [8674530](https://pubmed.ncbi.nlm.nih.gov/8674530/)
93. Bouret SG, Draper SJ, Simerly RB. Trophic action of leptin on hypothalamic neurons that regulate feeding. *Sci Signal*. 2004; 304: 108.
94. Yates BJ. Vestibular influences on the sympathetic nervous system. *Brain Res Rev*. 1992; 17: 51–59. PMID: [1638275](https://pubmed.ncbi.nlm.nih.gov/1638275/)
95. Yates BJ. Vestibular influences on the autonomic nervous system. *Ann N Y Acad Sci*. 1996; 781: 458–473. PMID: [8694435](https://pubmed.ncbi.nlm.nih.gov/8694435/)
96. Yates BJ, Bronstein AM. The effects of vestibular system lesions on autonomic regulation: observations, mechanisms, and clinical implications. *J Vestib Res*. 2005; 15: 119–129. PMID: [16179761](https://pubmed.ncbi.nlm.nih.gov/16179761/)
97. Vignaux G, Besnard S, Ndong J, Philoxène B, Denise P, Elefteriou F. Bone remodeling is regulated by inner ear vestibular signals. *J Bone Miner Res Off J Am Soc Bone Miner Res*. 2013; doi: [10.1002/jbmr.1940](https://doi.org/10.1002/jbmr.1940)
98. Denise P, Besnard S, Vignaux G, Sabatier JP, Edy E, Hitier M, et al. Sympathetic B antagonist prevents bone mineral density decrease induced by labyrinthectomy. *Aviakosmicheskaja Ekol Meditsina Aerosp Environ Med*. 2009; 43: 36–38.
99. Cheng JC, Guo X, Sher AH. Persistent Osteopenia in Adolescent Idiopathic Scoliosis: A Longitudinal Follow-Up Study. *Spine*. 1999; 24: 1218–1222. PMID: [10382248](https://pubmed.ncbi.nlm.nih.gov/10382248/)
100. Cheng JC, Guo X. Osteopenia in adolescent idiopathic scoliosis: a primary problem or secondary to the spinal deformity? *Spine*. 1997; 22: 1716–1721. PMID: [9259781](https://pubmed.ncbi.nlm.nih.gov/9259781/)
101. Cheng JCY, Qin L, Cheung CSK, Sher AHL, Lee KM, Ng SWE, et al. Generalized low areal and volumetric bone mineral density in adolescent idiopathic scoliosis. *J Bone Miner Res*. 2000; 15: 1587–1595. PMID: [10934658](https://pubmed.ncbi.nlm.nih.gov/10934658/)
102. Cheng JC, Tang SP, Guo X, Chan CW, Qin L. Osteopenia in adolescent idiopathic scoliosis: a histomorphometric study. *Spine*. 2001; 26: C1–C5.
103. Byl NN, Gray JM. Complex balance reactions in different sensory conditions: adolescents with and without idiopathic scoliosis. *J Orthop Res*. 1993; 11: 215–227. PMID: [8483034](https://pubmed.ncbi.nlm.nih.gov/8483034/)
104. Kouwenhoven J-WM, Vincken KL, Bartels LW, Castelein RM. Analysis of preexistent vertebral rotation in the normal spine. *Spine*. 2006; 31: 1467–1472. PMID: [16741456](https://pubmed.ncbi.nlm.nih.gov/16741456/)
105. Burwell RG, Freeman BJC, Dangerfield PH, Aujla RK, Cole AA, Kirby AS, et al. Etiologic theories of idiopathic scoliosis: neurodevelopmental concept of maturational delay of the CNS body schema (“body-in-the-brain”). *Stud Health Technol Inform*. 2006; 123: 72–79. PMID: [17108406](https://pubmed.ncbi.nlm.nih.gov/17108406/)
106. Jansen M. Physiological Scoliosis. *Br Med J*. 1912; 2: 1372–1373.
107. Janssen MMA, Kouwenhoven J-WM, Schlösser TPC, Viergever MA, Bartels LW, Castelein RM, et al. Analysis of preexistent vertebral rotation in the normal infantile, juvenile, and adolescent spine. *Spine*. 2011; 36: E486–491. doi: [10.1097/BRS.0b013e3181f468cc](https://doi.org/10.1097/BRS.0b013e3181f468cc) PMID: [21240053](https://pubmed.ncbi.nlm.nih.gov/21240053/)
108. Goldberg CJ, Dowling FE, Fogarty EE. Adolescent idiopathic scoliosis: is rising growth rate the triggering factor in progression? *Eur Spine J*. 1993; 2: 29–36. PMID: [20058445](https://pubmed.ncbi.nlm.nih.gov/20058445/)